IOSR Journal of Engineering (IOSRJEN) **www.iosrjen.org**
ISSN (e): 2250-3021, ISSN (p): 2278-8719
Vol. 08, Issue 12 (December. 2018), ||V (IV) || PP 49-59

Specialized switching-mode power supplies (SMPS) for photovoltaic and conventional LED lighting systems

Corneliu Lungănoiu, Laurențiu Fara, Dan Crăciunescu*, Florin Drăgan, Paul Sterian
Polytechnic University of Bucharest, Faculty of Applied Sciences
Academy of Romanian Scientists
**Corresponding Author: Dan Craciunescu*

Abstract: The great benefits that LED technology offers have convinced several international companies to study and adopt this technology for both indoor and outdoor LED lighting systems. On the other hand, their DC power supply requires non-linear switching-mode voltage sources to increase power efficiency. However, the SMPSs have some drawbacks, such as quality dropping of the electric power due to the absorbed current harmonics and their propagation through the grid. In this article, two types of design power supplies, for both indoor (conventional) and outdoor (photovoltaic) lighting applications, are proposed and analyzed. Special integrated circuits are used, namely HV9910B (buck-converter) for indoor lighting and HV9912B (boost-converter) for outdoor lighting. The circuit analysis required for obtaining the values of the scheme components is used to determine the main electrical parameters of LED lighting systems, such as power efficiency and power factor, as well as to highlight the best implementation schemes. The simulation of the circuits and parameter analysis are performed. Using the simulation results, an improved SMPS design approach for PV and conventional LED lighting systems can be designed, with certain advantages for practical applications.

Keywords: Hybrid switching-mode power supplies (SMPS), photovoltaic / conventional LED lighting systems, buck converter, boost converter

---

Date of Submission: 13-12-2018 Date of acceptance: 29-12-2018

I. INTRODUCTION

With the increase of the electricity generation capacities through environment-friendly methods (eg. by developing photovoltaic systems [1]), it is intended to optimize the electricity consumption by increasing the energy efficiency of devices, circuits and equipments. At the same time, it is necessary to consider the continuous increase of the electricity invoices. Thus, for a lighting system, the lifetime (5-20 years) costs are distributed as follows: 10% investment, 10% maintenance and 80% electricity [2]. Thus, although the higher cost of new technologies (photovoltaic systems, LED technology, switching power sources) appears to be an important drawback to their spread, from the perspective of the new lifecycle cost concept, they show real potential in both obtaining a high energy efficiency as well as important financial savings. LED lamps can be easily integrated into an autonomous lighting system based on photovoltaic systems, as power supplies, due to their low power consumption. Also, the fact that their performances are not affected by low temperatures require these lamps to be used in outdoor lighting systems. There are specialized LEDs studies regarding mathematical / physical models [3] and their technology [4], as well as their use within lighting systems [5]. The transition from linear (relatively simple and low-efficiency) power supplies to switching, non-linear (high efficiency and with a more complex electrical scheme) ones was gradually achieved, highlighting various topologies. The advantages of the switching power sources were analyzed in comparison with their classical variants, as well as their types, their uses and the most suitable schemes for each domain [6, 7]. Thus, a general approach to advanced DC-DC converters is discussed by Luo et. al. [8], while their applications to LED lighting systems (buck, boost, boost-buck and flyback converters), as well as practical details for the design and realization of such converters, are presented by Winder [9]. The influence of the parameters of the various active components (transistors) and passives (resistances, capacitors, coils) on the correct operation of the electronic scheme (for example, emphasizing the essential role of capacitors with an ESR - Equivalent Series Resistance) is analyzed by Tutak [10]. The stability of the proposed electronic schemes, as well as the selection criteria for the integrated control and control circuit, are discussed by Rahman [11]. Practical aspects of printed circuit board designs (PCBs) that take into account the electromagnetic interference (EMI) are illustrated by Winder [9]. The analysis of some power circuits for low power LEDs was developed by Farsakoglu et. al. [12], while Leung et. al. [13] presents

an analysis of a high power LED driver circuit. The study of Farsakoglu et. al. [14] reviews the factors that affect the efficiency of power LEDs and suggests specific power schemes. The analysis, design and electronic layout of a flyback converter for LEDs with power factor correction is discussed by Celik et al. [15].

In this study we analyze, design and characterize a power supply for a LED lighting system. Due to the fact that the reduced size of such a system does not allow the use of a bulky power supply, it was chosen a buck-converter source for indoor lighting systems, for which its operation mode was studied, as well as how to choose its components and the integrated circuit for electronic switch control. It is also proposed a boost-converter source for an outdoor photovoltaic system, where it was discussed how to achieve the electronic scheme, as well as the same tasks like in the previous case. Simulation of circuits and analysis of the main electrical parameters (efficiency, power factor) for the two schemes were performed using the specialized software MAPLAB Mindi.

II. THEORETICAL BACKGROUND

2.1 Analysis of the block diagrams of the two lighting systems

Two LED lighting systems, both indoor and outdoor (photovoltaic), are analyzed. The block diagrams of these lighting systems are shown in Figures 1 and 2.

In Figure 1, the EMC (Electro-Magnetic Compatibility) filter is followed by the Power Factor Correction (PFC) block. The specific topology of the buck converter is implemented by the DC-DC block and the output filter.

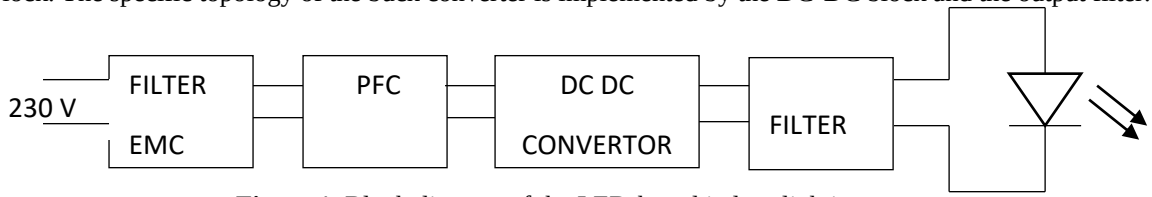

Figure 1. Block diagram of the LED-based indoor lighting system

Figure 2 shows the main controller that performs automatic switching between energy sources (PV system, electric battery or electrical network), as well as on/off switching of the lamp according to the signals received from the external sensor and the dedicated battery charge controller.

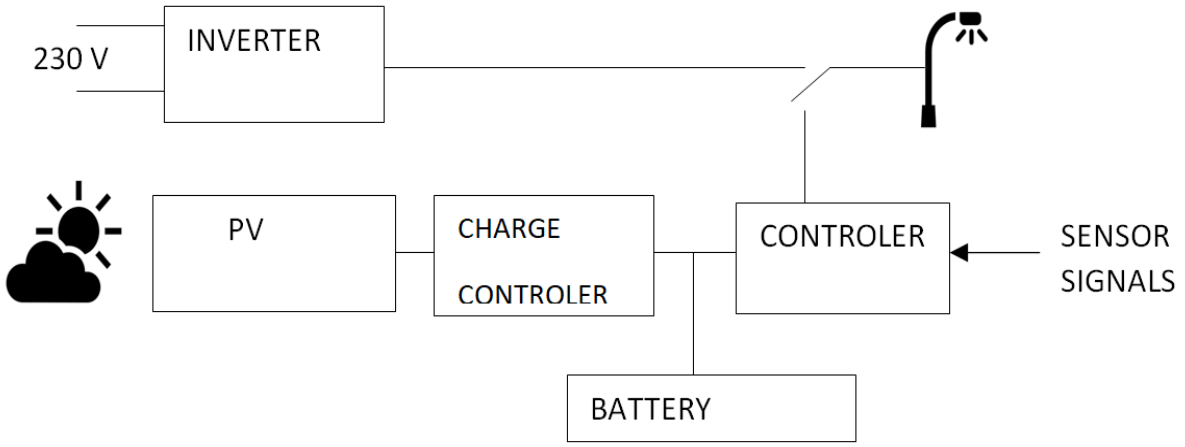

Figure 2. Block diagram of LED-based outdoor PV system

2.2 Mathematical model of the buck converter

The buck converter produces a voltage at the output whose mean value is less than the input voltages. It can operate in two modes: Continuous Conduction Mode (CCM) and Discontinuous Conduction Mode (DCM), however our analysis will be limited to CCM mode, specific to the considered application (LED power supply). The command switch is operated at a certain frequency and can produce a rectangular voltage with varying fill factor at the load terminals. In the following analysis, we have introduced several parameters: T_s - period of the command signal, f_s – frequency of the command signal, U_i - input voltage and U_0 - output voltage.

Figure 3 shows the electrical diagram of the buck converter and the characteristic waveforms describing its operation.

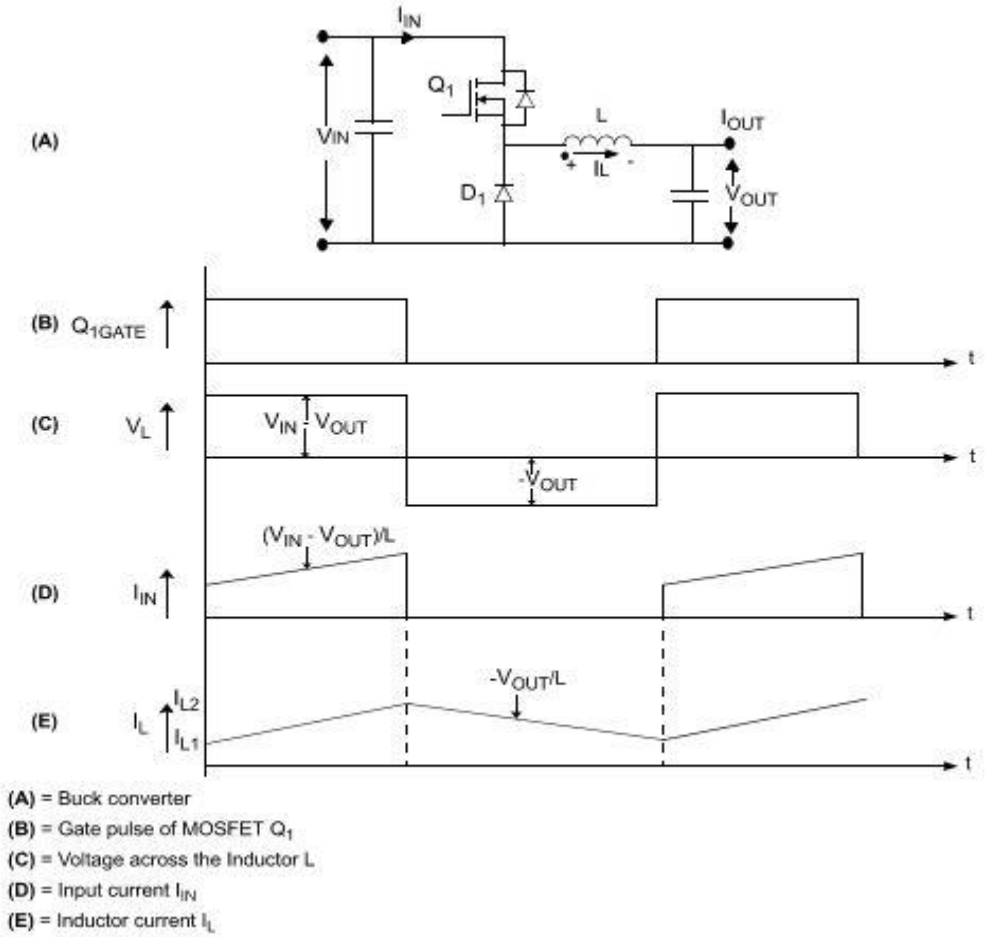

Figure 3. Buck converter and specific waveform [22]

If the switch is open for a time t_{ON} and locked for a t_{OFF} time such that $t_{ON} + t_{OFF} = T_s$ (cycle period), the fill factor will be:

$$D = t_{ON} / T_s \quad (1)$$

If we denote:

$$D' = t_{OFF} / T_s \quad (2)$$

the following relationship will be obtained:

$$D + D' = 1 \quad (3)$$

The conversion factor of this type of converter is:

$$M(D) = U_0 / U_i = D \quad (4)$$

The inductor sizing relationship is:

$$L = ((U_i - U_0)\, D\, T_s) / \Delta I_L \quad (5)$$

where ΔI_L is the peak to peak variation of the current through the coil around the average value of I. Also, if the peak to peak amplitude of the capacitor pulse is ΔU_0 then the following relationship allows the calculation of the output capacitor value:

$$C = (\Delta IL\ Ts) / (4\ \Delta U0) \quad (6)$$

2.3 Mathematical model of the boost converter

The boost converter is an insulated converter that produces an output voltage greater than the input one [16-21]. The electrical scheme and corresponding waveforms are shown in Figure 4.

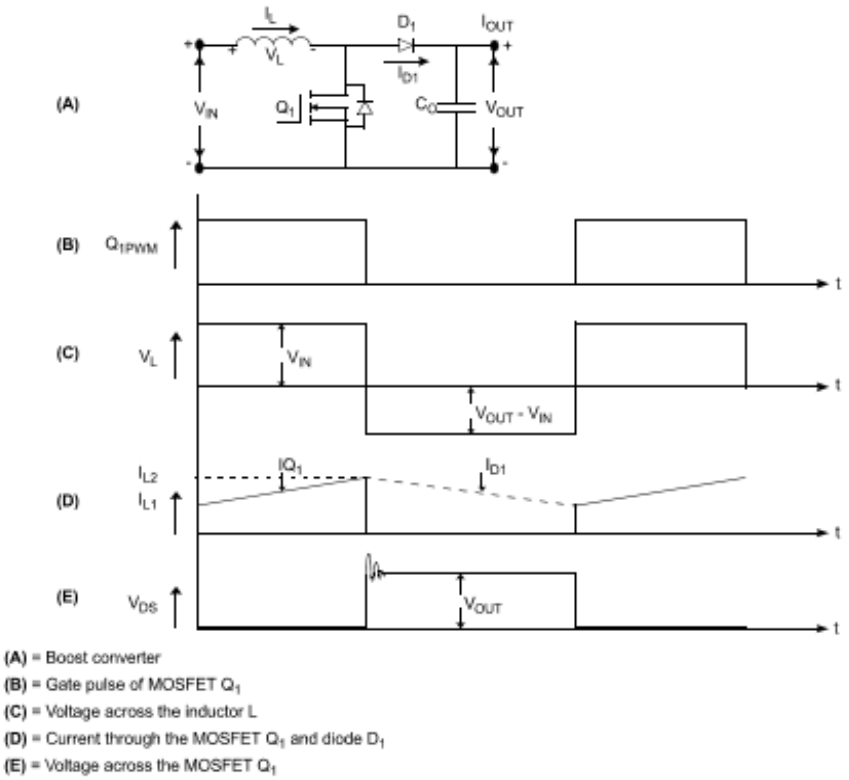

Figure 4. The boost converter electric scheme and the specific waveforms [22]

The conversion factor is given by

$$M(D)=U_0 /U_i =1/(1-D) \quad (7)$$

This relationship shows that the output voltage is greater than the input one. If R is the load resistance, then the average current I absorbed by the inductor from the power supply is given by:

$$I = U_0/((1-D)R)=U_i /((1-D)^2R) \quad (8)$$

The inductor sizing relationship is:

$$L=(U_i D T_s)/\Delta I_L \quad (9)$$

where ΔI_L is the peak to peak variation of the current through the coil around the average value of the current I. Also, the relationship of sizing the output capacitor is:

$$C=(U_0 D T_s)/(R \Delta U_0) \quad (10)$$

where ΔU_0 is the peak to peak amplitude of the pulse on the capacitor.

III. METHODOLOGY

3.1 Methodological concepts of buck and boost converters design

If the first LED that operated at a current of 350mA was available on the market in 1999, today there are many manufacturers that offer power LEDs working at currents of 700mA, 1A and even more. Our application requires a string of LEDs operating at $I_{0,max}$ = 350mA and direct voltages between $V_{0,\,min}$ = 30V and $V_{0,max}$ = 40V.

In the previous chapter, there were discussed the basics required to understand the operation of buck and boost converters. The control of the switching transistor is realized in the modern specialized integrated circuits. Many semiconductor companies produce such circuits, including Fairchild Semiconductor, Supertex Inc. or Microchip. One of the most popular circuits, the HV9910B [22], was proposed to be discussed in this article. This circuit effectively implements a buck converter that acts as a constant current driver for LEDs, with a minimum of external parts. Figure 5 presents the 8-lead SOIC (Small Outline Integrated Circuit), used for buck converter design.

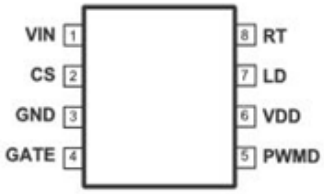

Figure 5. 8-Lead SOIC [23]

Figure 6 shows the internal block diagram of the HV9910B circuit, with the internal voltage regulator that provides power for internal circuits, the oscillator generating the transistor switching frequency, the 250 mV voltage reference, and the operational amplifiers to limit the current in LEDs .

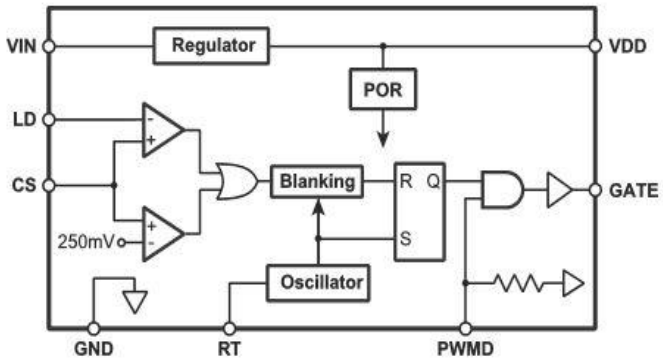

Figure 6. Internal block diagram from HV9910B [23]

The integrated amplifier HV9912, specially designed by Microchip for the boost, buck-boost and SEPIC (single-ended primary-inductor) converter, was chosen for the boost converter. As a design data we will consider an input voltage U_i = 12V with $U_{i,min}$ = 9V and $U_{i,max}$ = 14V, $U_{0,min}$ = 30V and $U_{0,\ max}$ = 40V, I_0 = 350mA, with a 10% dynamic LED impedance of 20Ω and n> 0.9.
Figure 7 shows a 16-lead SOIC (Small Outline Integrated Circuit) 16-Lead terminal block, used for boost converter design.

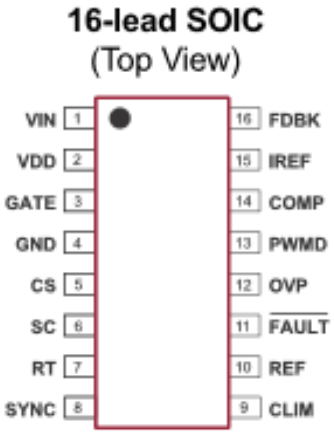

Figure 7. Pin significance for HV9912 [24]

Figure 8 shows the internal block diagram of the HV9912 circuit. The block diagram contains a 90 V voltage reference used for internal blocks, an internal oscillator, a synchronization input that allows multiple cascaded circuits to be connected, and a MOS transistor control input to limit the current through the LED.

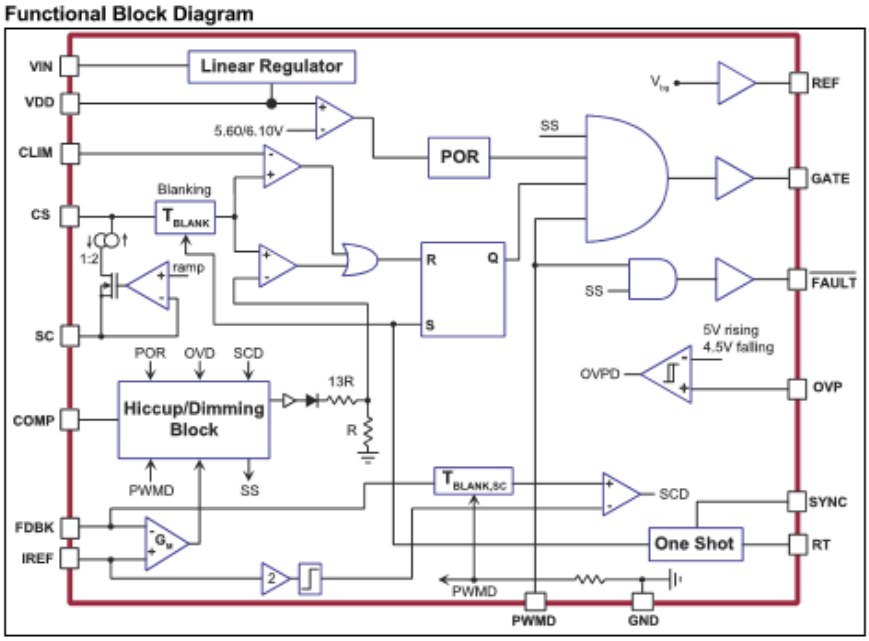

Figure 8. Internal circuit block diagram HV9912 [24]

3.2 The MAPLAB Mindi Software

The MAPLAB Mindi 20 software package [25] was used to simulate the two lighting systems studied in this paper. It is constituted as a simulator of analog circuits and integrates two modules:

1. SIMPLIS - Simulation of Piecewise Linear Systems - a circuit simulator designed specifically to simulate switching power converters.
2. SIMetrix - a tool containing a SPICE simulator, a scheme editor and a waveform viewer.

IV. RESULTS AND DISCUSSIONS

4.1. Buck converter design

The internal regulator from the diagram accepts at input (pin 1 - VIN) voltages between 8V and 450V, making it easier to use this circuit in both mobile and grid-powered applications. At pin 8 – RT, the external resistor required for the internal oscillator is connected, which can generate a frequency between 20kHz and 120kHz. Pin 4 - GATE, is the one that controls the gate of the switching transistor, while pin 2 - CS, is the one to which the resistance of the output current is connected, the voltage drop from its terminals being applied to the non-inverse input of the internal comparator. The manufacturer indicates in the circuit catalog sheets the use of a resistor of RT = 226 kΩ (R1 in the electrical diagram presented Figure 9) to obtain a frequency of 100kHz (i.e. T_s = 10 µs) and also a bypass capacitor at pin 6 – VDD, with a value of 2.2µF, 16V (C3 in Figure 9). Using the internal voltage of 250 mV, and considering a current ripple $I_{0,\,max}$ = 350 mA of maximum 15% (i.e. 30% peak at peak), the resistance R2 = 0.25 / (1.15 x $I_{0,\,max}$) = 0.62Ω [23].

If it is accepted the nominal voltage on the alternative voltage network as $V_{ac,nom}$ = 230V (with agreed variations between 90V and 265V), then the peak voltage, which is actually the voltage U_i of the formula (2.6), will be U_i = 21 / 2 x 230 = 325V. Substituting in relation (2.5), L = ((U_i - U_0) D T_s) / (2 Δi_L), T_s = 10 µs, 2 Δi_L = 0.3 x $I_{0,max}$ = 0.105 A, we obtain L = 3.34mH.

In the theoretical presentation of the buck converter it was shown that the maximum voltage that the transistor holds when blocked is the input voltage (with the worst case, the maximum value). When the transistor drives, diode D1 is the one that supports this voltage. We deduce that V_{FET} = V_{diode} = 1.5 x $2^{1/2}$ x $V_{0,maxAC}$ = 1.5 x $2^{1/2}$ x 265 = 562 V, where 1.5 is a safety factor. It was chosen a MOSFET transistor with 600 V, > 1A of type STD2NM60 and a fast diode of type STTH1R06 [9]. The same voltage and current requirements are also required for the rectifier bridge, which on the continuous voltage side will be completed with two capacitors C1 = 33µF, 450V for maintaining the continuous voltage and C2 = 330 nF, 450V to eliminate the high frequency disturbances produced by the converter. Also, to maintain the inrush current within reasonable limits (when connecting the supply voltage), a NTC thermistor of 120 Ω, 1 A is required. The electronic scheme of the buck converter is shown in Figure 9.

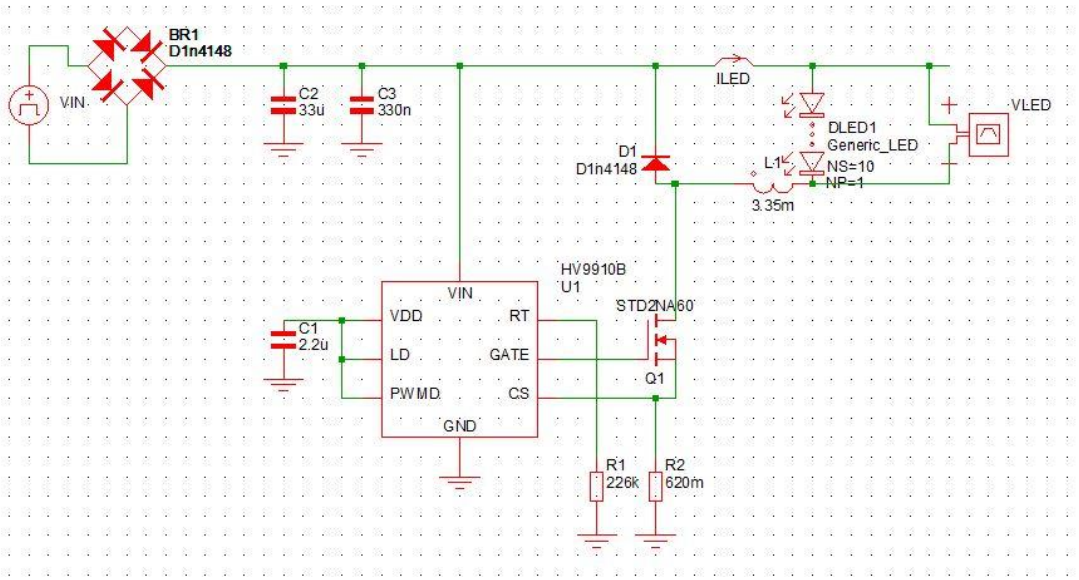

Figure 9. Electronic scheme of the buck converter

4.2 Boost converter design

The input voltage that can be applied to pin 1, VIN, is between 7.5V and 100V. Pin 10, REF, having a 0.1µF bypass capacitor connected to the ground, provides a reference voltage of 1.25V. Pin 2 - VDD, which provides the required voltage for the internal blocks of the integrated circuit, must also be connected to the ground via a capacitor with a small ESR of 2.2 µF. The RT resistor connected between pin 7 - RT and ground sets the constant frequency operating mode circuit. The manufacturer indicates the frequency calculation with RT = 1 / (f_s x 18pF) which for f_s = 100kHz leads to RT = 560kΩ. At 14 COMP pin, a RC compensation network, consisting of Rz = 22kΩ, Cz = 6.8 nF, Cc = 2.2 nF, is connected [9].

If we consider the minimum efficiency of the converter of 0.9, then the relation between the output and the input power, $V_{0,max}\ I_{0,max} = \eta\ V_{i,min}\ I_{i,max}$, allows the calculation of the maximum input current (which goes through the inductor). We conclude that $I_{i,max}$ = (40 x 0.35) / (0.9 x 9) = 1.73 A. Also, the filling factor D_{max} = 1-$V_{i,min}$ / $V_{0,max}$ = 1-0.9 x 9/40 = 0.7975. Accepting a current ripple through a 25% coil, it can be calculated the inductance value L = ($V_{i,min}$ D_{max}) / (0.25 $I_{i,max}$ f_s) = 165 µH. The MOS switch with N channel, connected to pin 3 – GATE, supports the maximum output voltage, $V_{0,max}$. Taking a 20% safety margin, we get VFET = 1.2 x 40 = 48V. The IFET current = $I_{i,max}$ x $(D_{max})^{1/2}$ gives an IFET value of 1.55A [9]. A 100V, 4.5A transistor is selected for this converter. At the same time, diode D1 supports the same maximum voltage V_{diode} = V_{FET} = 48V. A Schottky diode of 2A, 100V is chosen. The output voltage variation is $\Delta U_0 = R_{LED}\ \Delta I_0$ = 20 x 0,035 = 0,7V where we can deduce the output capacitance C3 = ($I_{0,\ max}$ D_{max}) / (f_s ΔU_0) = 3,9 µF. The integrated circuit allows for connection of a second transistor MOS to terminal 11 – FAULT, in the case of short-circuit to output or overvoltage. The manufacturer recommends a 100V, 0.7Ω and Q_g = 5nC transistor. Resistors R1 and R2 are traversed by the currents through the two transistors and the manufacturer's sizing relations are: R2=0.15W/$(I_{0,max})^2$=0.15/(0.35 x 0.35)=1.2Ω; R1=0.25V/(1.125$I_{i,max}$)= 0.25V/(1.125 x 1.73)=0.13Ω. The voltage divider connected between pin 10 – REF, pin 15 – IREF and GND can be dimensioned using the following equations: R3 + R4 = 1.25V / 50 µA = 25kΩ, respectively $I_{0,max}$ R2 = (1.25 R4) / (R3 + R4), resulting the following values: R4 = 8.5kΩ and R3 = 16.5kΩ. The current slope control through the inductor is realized by the resistors R7 and Rslope. The calculation relation is: R_{slope} = (10 R7 f_s L) / (($V_{0,\ max}$ - $V_{i,\ min}$) R1). Since the manufacturer recommends that the value for R7 be in the range of 25 kΩ – 50 kΩ, for R7 = 1 kΩ we obtain R_{slope} = 41kΩ. The voltage divider R5 and R6, connected between pins 10, REF, 9, CLIM and GND, performs the current limitation through the inductor. The voltage at pin 9 is V_{clim} = 1.35 $I_{i,max}$ R1 + 4.5 R7 / R_{slope} = 0.4V. Since R5 + R6> 1.25V / 50 µA = 25kΩ we choose R5 = 20kΩ and R6 = 10 kΩ. Finally, the resistors R8 and R9 form the resistive divider connected to pin 12, OVP achieves protection of the LED string against overvoltages. Considering V_{open} = 1.2$V_{0,max}$ = 48V, we calculate R8 = (V_{open}-5) 2 / 0.1 = 18.5kΩ and R9 = 5R8 / (V_{open}-5) = 2.2 kΩ. Capacitors C1 = C2 = 2.2µF, 50 V perform a reduced impedance path for high disturbance frequencies thrown along the supply line. Figure 10 shows the full electronic scheme of the boost converter.

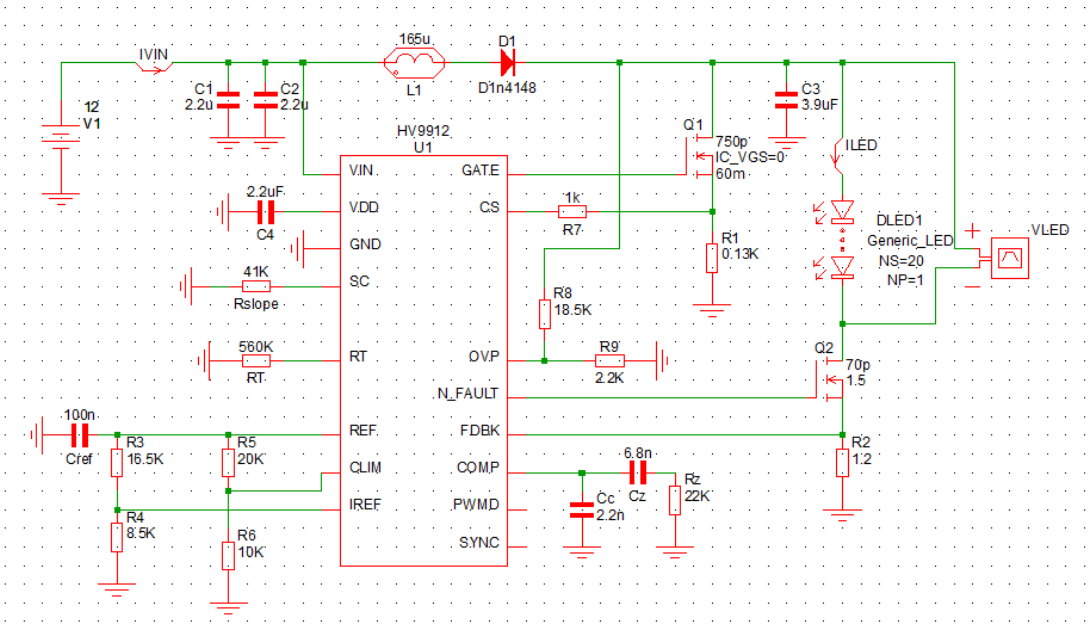

Figure 10. Electronic scheme of the boost converter

4.3. Simulated results and discussions for the conventional lighting system

Using the Simetrix module of the specialized software MapLab Mindi 2.0, it was obtained the evolution over time of the current and voltage in the LEDs for the buck converter of the conventional lighting system (Figure 11). It is noted that after a 12 ms time interval, the stationary values of the current and voltage in the LEDs are obtained.

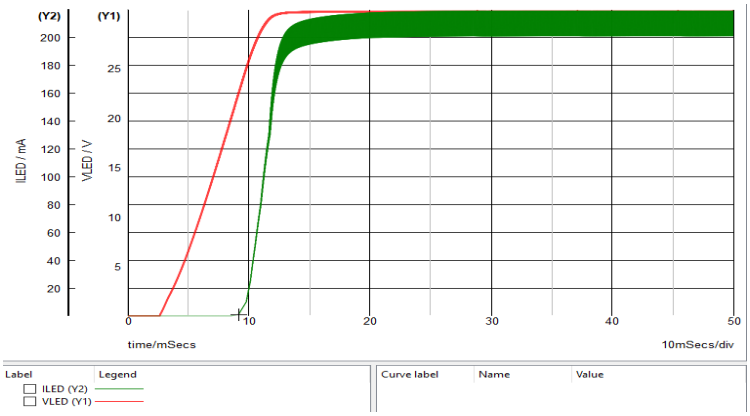

Figure 11. The evolution over time of current (I_{LED}) and voltage (V_{LED}) for the buck converter of the conventional system

The evolution over time of the current through the buck converter was obtained for two different time scales, respectively in the order of milliseconds (Figure 12) and microseconds (Figure 13). The fluctuations of the current through the coil are highlighted in the two analyzed cases.

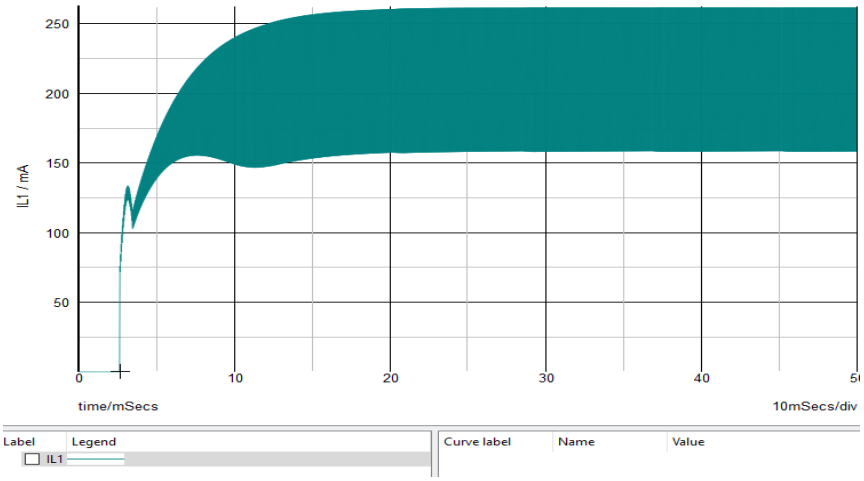

Figure 12. Evolution of current through the coil for a millisecond scale

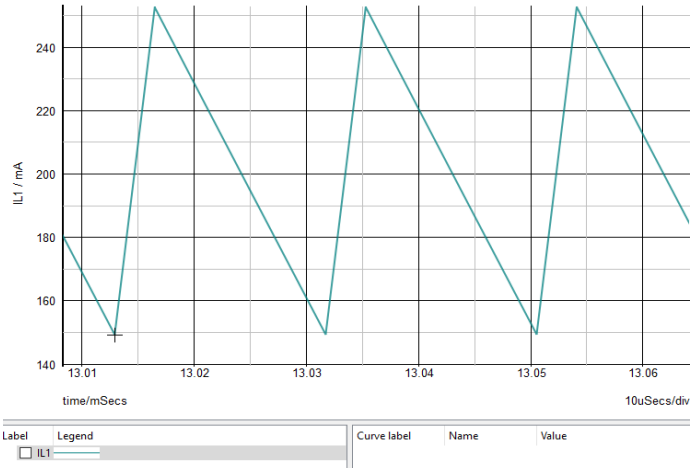

Figure 13. Evolution of current through the coil for a microsecond scale

The results obtained through simulations are useful for understanding the normal operation of the conventional buck converter system.

4.4. Simulated results and discussions for the PV lighting system

Using the SIMPLIS module from the specialized MapLab Mindi 2.0 software, it was obtained the evolution of the current in LEDs for the boosting PV converter system (Figure 14). It is found that, after a time interval of 16,8 ms, the stationary state of the LED is shown, indicating a current drop in the range 16.3 - 16.5 ms. There is a variation of the current in LEDs of about 15 mA.

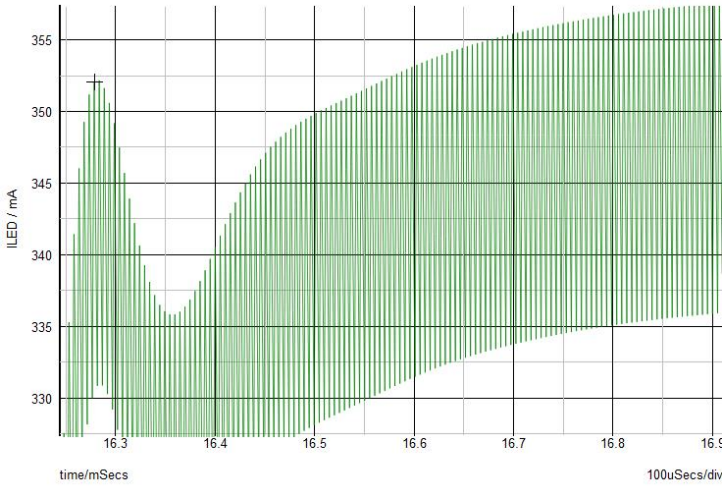

Figure 14. The evolution of LED current (I_{LED}) over time for the boost system of the PV system

At the same time, simulations allowed fluctuations of current in the coil to be highlighted over a range of 0.07 μs, between 16.67 μs and 16.74 μs (see Figure 15).

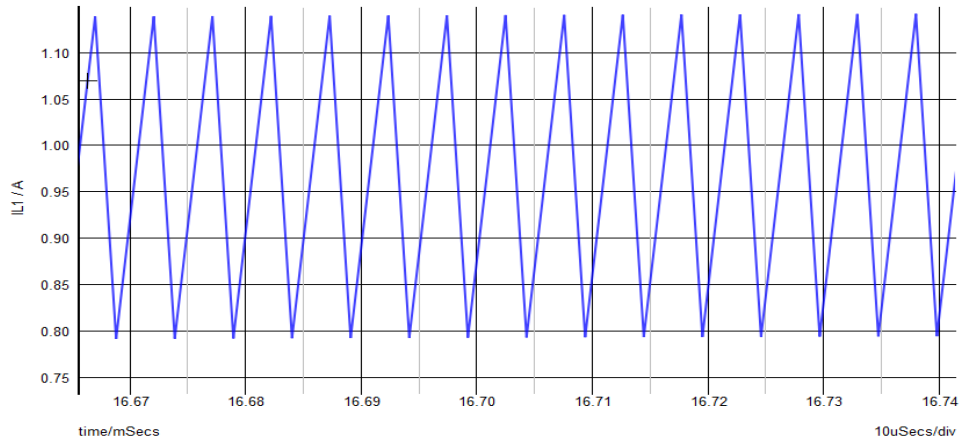

Figure 15. The time evolution of the current through the coil for a microsecond scale for the boost converter

In order to establish the proper functioning of the PV protection system with a boost converter type, the voltage simulation on the COMP pin of the integrated circuit was carried out over a 20 ms interval, as seen in Figure 16. It was found that the specific voltage form on this pin that can be used in system maintenance operations.

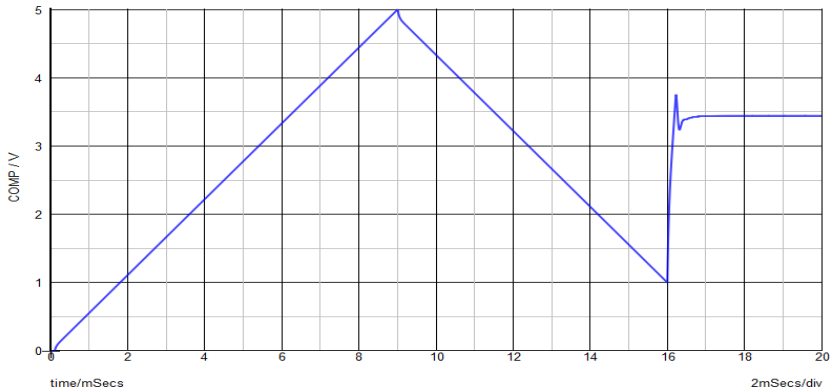

Figure 16. The voltage on the COMP terminal of the integrated circuit

V. CONCLUSIONS

The study yielded some useful results for the design of conventional and PV LED lighting systems, consistent with those set forth in the literature [4-15], as follows:

-Two schemes of switching-mode power supplies (SMPS) for indoor and outdoor LED lighting systems (conventional and PV), based on buck and boost converters, were conceived and analyzed.

-There were discussed operational methods for obtaining the electronic schemes and for checking the parameters and validating their behavior using specific software applications.

-There have been highlighted the commercially favorable aspects that can be obtained by the unitary approach of conventional LED lighting systems, respectively non-conventional PV systems.

ACKNOWLEDGEMENT

This work was conducted under: (1) the research project SOLHET, 2016–2019, M-ERA.Net program, supported by the Romanian Executive Agency for Higher Education, Research, Development and Innovation Funding (UEFISCDI), project no. 34/2016; (2) the project MultiscaleSolar MP1406, 2015–2019, supported by the European Commission through COST program.

REFERENCES

[1]. Fara, L.*Physics and technology of solar cells and photovoltaic systems (in Romanian)*. AOSR Publishing House, Bucharest, 2009

[2]. Golovanov, N.et. al.. *Energetic efficiency. Environment. Modern economy(in Romanian).*AGIR Publishing House, Bucharest, 2017

[3]. Sterian, P. *Photonics (in Romanian).* Printech, Bucharest, 2000
[4]. Held, G. *Introduction to Light Emitting Diode Technology and Applications.* CRC Press, 2009
[5]. Mottier, P. *LEDs for Lighting Applications*. John Wiley & Sons, 2009
[6]. Pressman, A. *Switching Power Supply Design*. McGraw-Hill, 1998
[7]. Erickson, R.W., Maksimovic, D. *Fundamentals of Power Electronics*. Kluwer Academic Publishers, 2002
[8]. Fang, L. L, Hong, Y. *Advanced DC/DC Converters*. CRC Press, 2004
[9]. Winder, S. Power Supplies for LED Drivers. Elseiver Inc., 2008
[10]. Tutak, A. *LED Technologies in Energy Efficient Applications*, M.Sc. Dissertation, Izmir, 2009
[11]. Rahman, M. S. *Buck Converter Design Issues*, M.Sc.Dissertation, Linkoping, 2007
[12]. Farsakoglu, O. F., Hasirici, H.Y. *Energy optimization of lower power LED drivers in indoor lighting.* Journal of Optoelectronics and Advanced Materials, vol. 17, No. 5-6, May-June 2015, p. 816-821
[13]. Leung, W.Y., Man T. Y., Chan, M. *A High-Power-LED Driver with Power-Efficient LED- Current Sensing Circuit*, IEEE 2008
[14]. Farsakoglu, O.F., Atik, I. *Analysis of the factors affecting operation and efficiency of power LED drivers and circuit design*. Optoelectronics and Advanced Materials-Rapid Communications, vol. 9, No. 11-12, Nov.- Dec. 2015, p. 1356-1361
[15]. Celik, I., Farsakoglu, O.F., Nalbantoglu, M. *The design and analysis of LED drivers with power factor correction in lighting applications*. Optoelectronics and Advanced Materials-Rapid Communications, vol. 11, No. 3-4, March- April. 2017, p. 251-261
[16]. Popescu, V*Power Electronics (in Romanian)*. West Publishing House, Timișoara, 2005
[17]. Alexa, D., Ionescu, F., Gâtlan, L., Lazăr, A. *Power converters with resonant circuits (in Romanian).*Technical Publishing House, Bucharest, 1998
[18]. Murmu, M. S., Sharma B, Mr. SSPM. *Study and design, Simulation of PWM based Buck converter for Low Power Application*. IOSR Journal of Electrical and Electronics Engineering, vol. 10, Issue 4 Ver. II, July-Aug 2015
[19]. Tăut, A. C. *Modulation for converters in commutation (in Romanian)*. PhD thesis. Cluj-Napoca Technical University, 2011
[20]. Stoica, I., Radu, A. I., Rogobete, M. *Power Electronics (in Romanian)*. Matrix Rom, Bucharest, 2015
[21]. Popescu, V., Negoițescu, D., Lascu,D.*Power converters in commutation*. West Publishing House, Timișoara, 1999
[22]. Application Note – *AN1114, 2007*. Retrieved from https://www.microchip.com
[23]. DataSheet-HV9910B–*DS20005344*,2015.Retrieved from www.microchip.com
[24]. DataSheet-HV9912–*DS20005583*,2016.Retrieved from www.microchip.com
[25]. www.microchip.com

Corneliu Lungănoiu et al "Specialized switching-mode power supplies (SMPS) for photovoltaic and conventional LED lighting systems." .IOSR Journal of Engineering (IOSRJEN), vol. 08, no. 12, 2018, pp. 49-59.